The following publication P. Chen, Y. Lin, H. Zeng, Y. Fang, Z. Xie and F. C. M. Lau, "Optimization of Hierarchical-Modulated and LDPC-Coded BICM With Physical-Layer Network Coding," in IEEE Internet of Things Journal, vol. 11, no. 21, pp. 35036-35047, 1 Nov.1, 2024 is available at https://doi.org/10.1109/JIOT.2024.3433489.

Optimization of Hierarchical Modulated and LDPC-coded BICM with Physical-layer Network Coding

Pingping Chen, Senior Member, IEEE, Yuchen Lin, Hanxin Zeng, Yi Fang, Senior Member, IEEE, Zhaopeng Xie, and Francis C. M. Lau, Fellow, IEEE

Abstract—In this paper, we investigate the performance of physical-layer network coding (PNC) with hierarchical modulation (HM) over a two-way relay channel (TWRC). While Gray mapping is the optimal for bit-interleaved coded modulation (BICM) systems in point-to-point communications, the superimposed constellation at the relay in PNC transmission does not maintain the same characteristics as the original Gray mapping at the users. Thus, to address this issue and obtain the optimal mapping for PNC, we propose a Pseudo-Gray (Pe-Gray) constellation for user-end hierarchical quadrature amplitude modulation (H-QAM). In particular, we develop the design criterion for the user constellation to avoid demodulation ambiguity and more importantly, to ensure that the superimposed constellation can be Gray-mapped. The achievable rate analysis and simulation results show that the proposed Pe-Gray can achieve significant performance gains of up to 2 dB over the conventional Gray, M3, and MSED constellations in powerimbalanced HM-BICM-PNC. The performance superiority of the Pe-Gray is further demonstrated over the power-imbalanced channels, which also suggests its enhanced robustness in wireless fading channels.

Index Terms—Hierarchical modulation (HM), physical-layer network coding (PNC), two-way relay channel (TWRC).

I. INTRODUCTION

PHYSICAL-LAYER network coding (PNC), originally proposed in [1], [2], can significantly increase the throughput of multi-user wireless communication networks. As a typical communication scenario, two-way relay channel (TWRC) allows bidirectional information exchange between two users via an intermediate relay, when the two users cannot reach each other directly [1]–[5]. Generally, PNC-aided TWR-C transmissions consist of two phases, i.e., multiple access (MAC) phase and broadcast (BC) phase. In the MA phase,

This work was supported by the National Natural Science Foundation of China (Grant No. 62171135, 62322106), Fujian Distinguished Talent Project (2022J06010), a RGC Research Impact Fund from the Hong Kong SAR, China (Project No. R5013-19), Fujian Province Key Technique Project (2023XQ004), and the Guangdong Basic and Applied Basic Research Foundation under Grant 2022B1515020086 (corresponding author: Yi Fang).

- P. Chen, Y. Lin, and H. Zeng are with the School of Physics and Information Engineering, Fuzhou University, Fujian 350002, China (e-mail: ppchen.xm@gmail.com, lyc_yuchen@163.com, hanxin.zeng@foxmail.com).
- Y. Fang is with the School of Information Engineering, Guangdong University of Technology, Guangzhou and also with the Department of Information Engineering, Fuzhou University 350002, China (e-mail:fangyi@gdut.edu.cn).
- Z. Xie is with the School of Advanced Manufacturing, Fuzhou University 362251, China (e-mail: xzp_fzu.edu.cn).
- F. C. M. Lau is with the Department of Electronic and Information Engineering, Hong Kong Polytechnic University, KowLoon, Hong Kong (e-mail: francis-cm.lau@polyu.edu.hk).

two users transmit signals to the relay simultaneously. The relay aims to decode the superimposed signals from two users into network coded (NC) messages, which are broadcasted to the users in the broadcast BC phase. The simplest form of the NC messages is a bit-wise exclusive-or (XOR) of the two user messages [6], [7]. There have also been studies investigating PNC systems with higher-order modulations beyond BPSK [4], [5].

As a high-order modulation for unequal error protection (UEP), hierarchical modulation (HM) can utilize a constellation of non-uniformly spaced signal points by its layered structure [8], [9]. Thus, HM technique has been widely studied in various communication scenarios, such as multiclass data transmissions [10], relay systems [11], [12], digital broadcast systems [13], and cooperative communications [14]. In HM constellations, the more significant bits in the symbol have a larger minimum Euclidean distance than the less significant bits. To achieve reliable transmission, HM-aided bitinterleaved coded modulation (BICM) [15] was introduced (HM-BICM) with spatially coupled (SC) protograph lowdensity parity-check (LDPC) codes [16], [17]. Recently, in relay communications over a TWRC, the PNC with HM (HM-PNC) was proposed and the end-to-end symbol error rate (SER) performance of the this system was derived [18]. For downlink asymmetric TWRC, [19] developed an efficient HM-PNC to improve the performance in the best link, while maintaining the performance of worst link.

In PNC systems, given a modulation at the users, the symbol mapping mainly determines the demodulation performance of the superimposed constellation at the relay. Note that in the superimposed constellations, one point may be associated with multiple pairs of two user constellation points, which may cause mapping ambiguity and then degrade the performance [4]. To address this issue, a non-uniform pulse amplitude modulation (PAM) was developed [20], where spacing between PAM constellation points is modified to avoid mapping ambiguity. On the other hand, with respect to phase-shift keying (PSK) modulation, [21] found the necessary and sufficient condition on a user bit mapping and introduced Semi-Gray mapping to improve system performance. Considering noisy transmissions in both MAC and BC phases, [22] proposed the optimal PAM binary-bit mappings. Furthermore, the performance of linear PAM-based PNC was investigated via a systematic analysis over power-imbalanced channels [23]. To ensure the reliability of the communication, the LDPC codes

© 2024 IEEE. Personal use of this material is permitted. Permission from IEEE must be obtained for all other uses, in any current or future media, including reprinting/republishing this material for advertising or promotional purposes, creating new collective works, for resale or redistribution to servers or lists, or reuse of any copyrighted component of this work in other works.

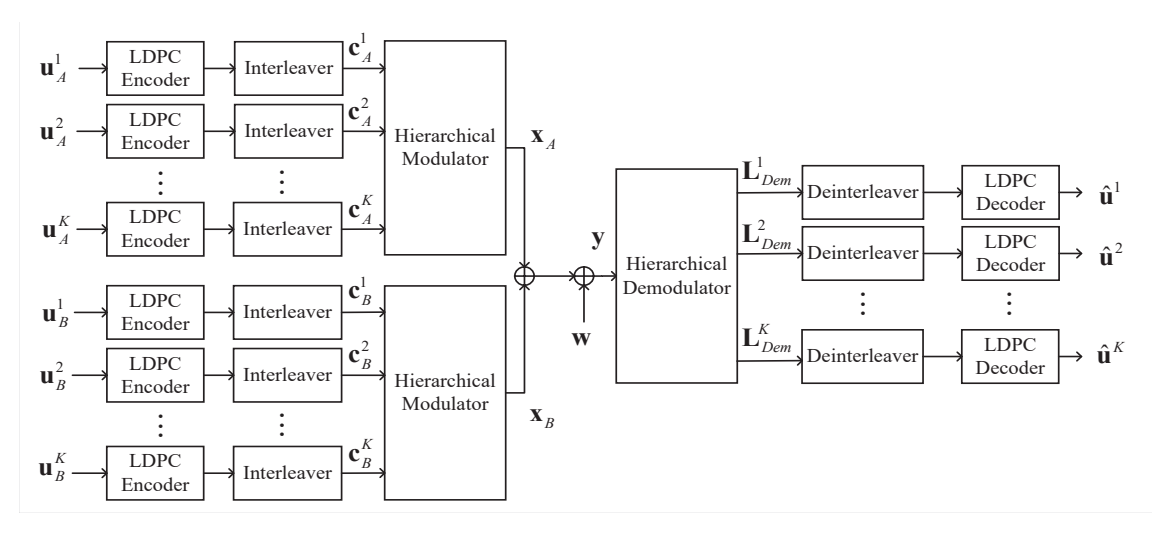


Fig. 1. Block diagram of LDPC-coded HM-BICM-PNC.

[24] have been extensively studied in PNC systems [25]—[28]. However, although there are existing constellation design methods for PNC systems with high-order modulation [20] and [21], it is still not clear how to design the optimal constellation for QAM-based HM-PNC. In point-to-point communications, Gray mapping is considered as optimal for BICM systems [15]. Similarly, the user-end constellation that ensures the superimposed constellation to be Gray mapped is seen as optimal in HM-BICM-PNC.

In this paper, we propose a constellation design of hierarchical quadrature amplitude modulation (H-QAM) for LDPCcoded BICM-PNC (HM-BICM-PNC). Since the superimposed constellation at the relay mainly determines the demodulation performance, the mapping at the users can be carefully designed. The proposed method aims to avoid mapping ambiguity at the relay, while ensuring that the superimposed constellation differs in only one bit between two adjacent points. As a result, the user-end QAM constellation may not be strictly Gray-mapped, i.e., Pseudo-Gray (Pe-Gray), but the superimposed constellation can be Gray-mapped. To achieve this, we first derive the labeling mapping design criterion for Pe-Gray constellation and show that this user-end mapping can generate the Gray-mapped superimposed constellation at the relay. Then, we find that both the constellation mappings and the constellation priority parameters of HM have significant impact on the performance of HM-BICM-PNC. The proposed Pe-Gray mapping is analyzed and show a higher achievable rate than the conventional Gray [29], MSED [30] and M3 [31] mappings in the HM-BICM-PNC. This result is finally verified by simulation results that the proposed Pe-Gray mapping outperforms the latter ones in terms of BER performance.

The remainder of this paper is organized as follows. Section II gives the system model of HM-BICM-PNC and introduces the 4/16-QAM HM scheme. In Section III, we elaborate the proposed design of Pe-Gray constellation and prove the properties of the superimposed constellation. Section IV shows the analytical and simulation results of HM-BICM-PNC systems. Finally, Section V summaries the main conclusions of the paper.

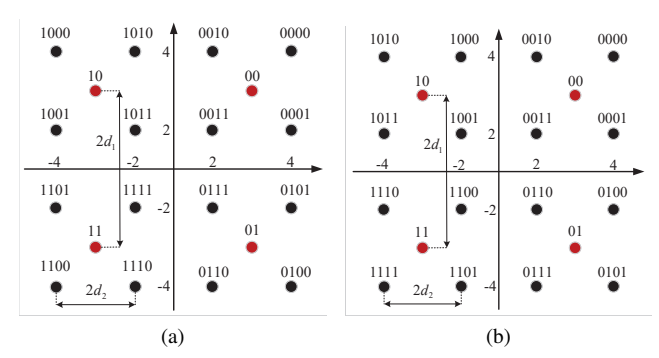


Fig. 2. HM diagram of 4/16-QAM modulation. (a) Gray. (b) Pe-Gray.

II. RELATED BACKGROUND

A. HM-BICM-PNC System Model

In this paper, we use x to denote a vector and x_i to denote the i-th element in x. The system model of a LDPC-coded HM-BICM-PNC scheme is shown in Fig. 1. As can be seen, the incoming information stream of user $t, t \in \{A, B\}$, is divided into $K = (\log_2 M)/2$ types of information bit streams. For k = 1, 2, ..., K, \mathbf{u}_{t}^{k} denotes the k-th layer bit stream for user t. Similar to [17], [30], we adopt multiple encoders and bit interleavers for different data streams. It can facilitate UEP for these coded data streams. Each of the K different information bit streams is encoded by an individual LDPC encoder to yield its corresponding coded-bit stream, respectively. These K types of coded-bit streams are then permuted by their respective bit-level interleavers to obtain \mathbf{c}_t^k , $k = 1, 2, \dots, K$. Every $m = \log_2 M$ consecutive coded bits output from the K interleavers are grouped together and modulated into an Mary transmitted signal x_t using a HM modulator. It should be noted that the coded bit streams output from the interleaver of each layer are assumed in layer order to be from the highest priority data stream to the lowest priority data stream, which are sequentially mapped to the most significant bit (MSB) positions to the least significant bit (LSB) positions in the symbol mapping, respectively. The labeling bit sequence of a modulated symbol is divided into $(\log_2 M)/2$ groups in a sequential order and the k-th group contains two labeling bits, $k=1,2,\ldots,(\log_2 M)/2$. The labeling bits within the k-th group is associated with the k-th MSB positions. This process results in a modulated symbol sequence for each user. Then, the received signal at the relay is the superimposed signal from the two users, given by

$$\mathbf{y} = h_A \mathbf{x}_A + h_B \mathbf{x}_B + \mathbf{w},\tag{1}$$

where h_A and h_B denote the power gains between users and relay that are known at the receiver, which can be accurately estimated by the blind channel estimation proposed in [32], [33]. w represents the complex Gaussian noise with zero mean and variance $N_0/2$ in each dimension. E_s/N_0 denotes the SNR per symbol, and E_s stands for the average energy per symbol. Unless specified otherwise, we assume equal power transmission, i.e., $h_A = h_B = 1$.

At the receiver side, we deal with the received signal by a hierarchical serial-parallel concatenated structure, consisting of a single-input-multiple-output (SIMO) hierarchical demodulator and K single-input-single-output (SISO) decoders. To be specific, given a received signal, the demodulation log-likelihood ratios (LLRs) output from the hierarchical demodulator can be passed to their corresponding k-th deinterleaver through a serial-to-parallel operation, $k=1,2,\ldots,K$. The LLRs are then deinterleaved and input into the corresponding LDPC decoder to produce the decoded output $\hat{\mathbf{u}}^k$, $k=1,2,\ldots,K$. Note that the log-domain maximum a posteriori probability (Max-Log-MAP) algorithm [34] and log-domain belief-propagation (log-BP) algorithm [35] are adopted for the hierarchical demodulator and K decoders, respectively.

B. 4/16-QAM Hierarchical Modulation

To ease the understanding of the HM process, Fig. 2(a) illustrates an example of hierarchical 16-QAM Gray constellation. The red dots represent four constellation points of a fictitious 4-QAM constellation, referred to as high-priority (HP) hierarchy, and the distance between the symbols in this hierarchy is denoted by $2d_1$. The actual transmitted symbols are represented by the black dots that form the hierarchical 16-QAM constellation as the low-priority (LP) hierarchy, where the distance between the symbols of the LP hierarchy in a quadrant is denoted by $2d_2$. Given a 4/16-QAM constellation with four bits, two HP bits and two LP bits are modulated into a symbol. The MSB bits, i.e., HP bits, offer superior protection against noise interference, ensuring decoding performance at all receivers. In contrast, the LSB bits, i.e., LP bits, provide lesser protection against noise and can only be decoded correctly at high SNR region [18], [30]. The parameter λ_1 is the priority of the 4/16-QAM constellation and is calculated as $\lambda_1 = d_2/d_1$. By adjusting λ_1 , we can modify the UEP of both the HP and LP streams. For instance, if $\lambda_1 = 0$, the 16-QAM constellation is reduced to 4-QAM, and only one HP stream remains. On the other hand, if $\lambda_1 = 1/2$, the 16-QAM constellation becomes uniform. In most HM-PNC systems, λ_1 typically ranges from 0 and 1/2.

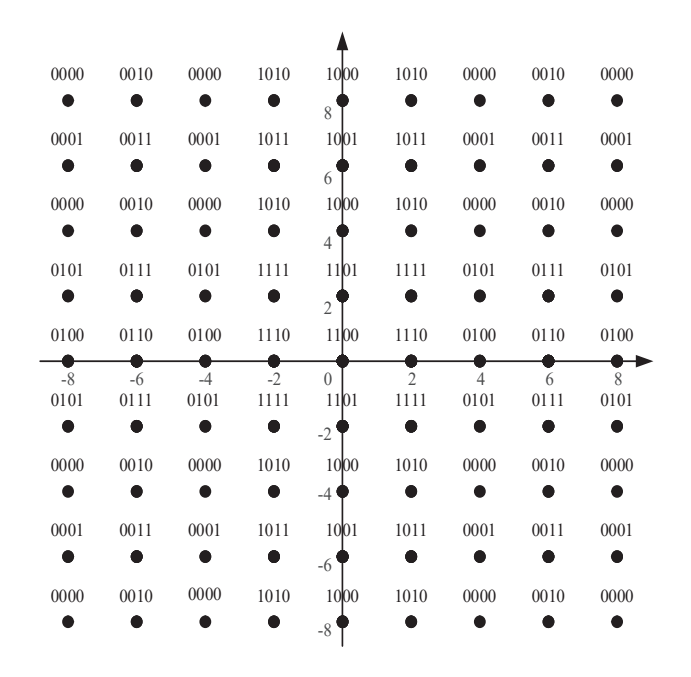


Fig. 3. Constellation diagram of $C_R(Gray)$.

III. PROPOSED CONSTELLATION AND ANALYSIS

A. Proposed Pe-Gray Constellation

In point-to-point communication systems, the Gray constellation is seen as the optimal mapping for BICM systems over AWGN channels [30], [36]–[38]. However, with respect to the PNC systems, given a constellation at the users, the superimposed constellation at the relay may not maintain the same characteristic as that at the users. Inspired by this, we propose a design of the HM constellation mapping to ensure that the superimposed constellation can be Gray-mapped, while the constellation at the users is Pseudo-Gray (Pe-Gray) mapping.

Let $C_R(\mathbf{C})$ denote the superimposed constellation at the relay when two users adopt the mapping C. We illustrate 4/16-QAM constellation of HM used for PNC system as an example. Fig. 3 shows the constellation with $\lambda_1=1/3$ superimposed from the Gray constellation in Fig. 2(a). We can see that the superimposed constellation is no longer the Gray mapping as in the user sides. Thus, to achieve Graymapped superimposed constellation at the relay, Fig. 2(b) presents a possible implementation of the 4/16-QAM Pe-Gray constellation at the users.

In the HM-BICM-PNC with 4/M-QAM modulations, the constellation is partitioned into K layers to support K types of data streams. The first layer is called the *base layer* and all other layers are called *enhancement layers*. The basic constellation is a 4-QAM Gray constellation with the center at (0,0). The layer-k data stream is represented by a layer-k basic constellation matrix denoted by $Q^k(d_k)$, $k=1,2,\ldots,K$ and d_k represents the distance between two neighboring constellation points in the constellation, $d_1>d_2>\cdots>d_{K-1}>d_K$. Moreover, we can see that there are eight different 4-QAM

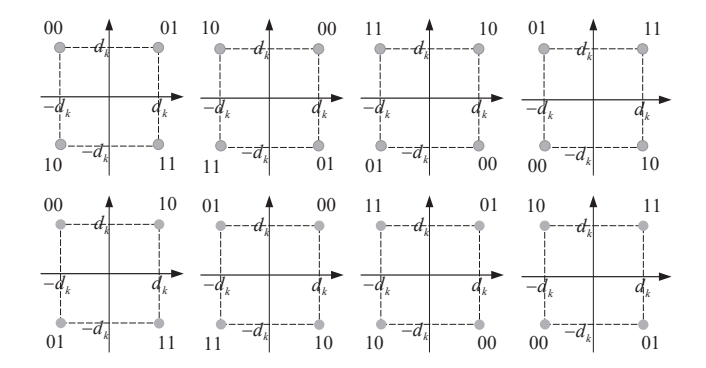


Fig. 4. The eight forms of the 4-QAM Gray constellation for $Q^k(d_k)$.

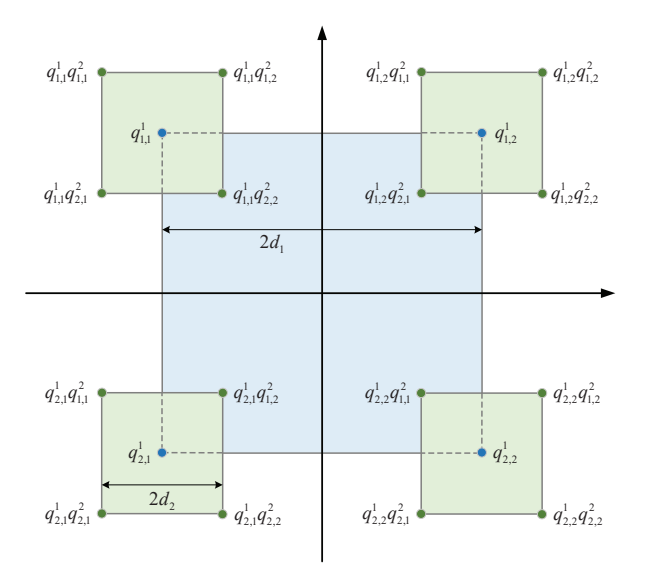


Fig. 5. Pe-Gray constellation for 4/16-QAM.

Gray constellation for each $Q^k(d_k)$, as illustrated in Fig. 4. Then, $Q^k(d_k)$ can be expressed as

$$Q^{k}(d_{k}) = \begin{bmatrix} q_{1,1}^{k}(-d_{k}, d_{k}) & q_{1,2}^{k}(d_{k}, d_{k}) \\ q_{2,1}^{k}(-d_{k}, -d_{k}) & q_{2,2}^{k}(d_{k}, -d_{k}) \end{bmatrix}, (2)$$

where $q_{i,j}^k(x_{i,j},y_{i,j})$ is the constellation point in the i-th row and j-th column of $Q^k(d_k)$, labeled with $q_{i,j}^k \in \{00,01,10,11\}$ and identified by its coordinates $(x_{i,j},y_{i,j})$, where $x_{i,j},y_{i,j} \in \{-d_k,d_k\}$ and $i,j \in \{1,2\}$.

The 4/M-QAM Pe-Gray constellation can be constructed sequentially using $Q^k(d_k)$, $k=1,2,\ldots,K$. We use a matrix V^k to represent a $4/4^k$ Pe-Gray constellation, which is generated by the basic constellation matrices from the previous k layers, $k=1,2,\ldots,K$. The constellation point in the i-th row and j-th column of V^k is labeled with a vector of k groups $\mathbf{v}_{i,j}^k = \left\{v_{i,j}^1, v_{i,j}^2, \cdots, v_{i,j}^k\right\}$, where each group contains 2 bits $v_{i,j}^h \in \{00,01,10,11\}$, and $h=1,2,\ldots,k$. The labeling bits in the k-th group correspond to the k-th MSB positions. The detailed design rule for the Pe-Gray constellation is given next.

1) Gray-Mapped Base Layer: The base layer constellation, i.e., the first layer, is represented by a matrix $V^1 = Q^1(d_1)$. It contains four constellation points with $\mathbf{v}_{i,j}^1 = \{v_{i,j}^1\}$ that is determined by $Q^1(d_1)$, $i,j=\{1,2\}$. The constellation is

equally divided into 4 quadrants, which are referred to as layer-1 quadrants.

2) Structured Gray-Mapped Enhanced Layers With Identical Mapping Orders: From the viewpoint of layer-1 quadrant, the second group of labeling bits in the 4/16-QAM Pe-Gray constellation consists of four Gray mappings. These mappings share identical mapping orders for the 4 quadrants within the complex plane. An example of a 4/16-QAM Pe-Gray constellation is presented in Fig. 5, where the blue plane denotes the base layer constellation, and the green plane denotes the enhanced layer constellation, which is shifted to the location of the four constellation points of the base layer to generate new constellation points. For 4/16-QAM modulation, the actual transmitted symbols are green constellation points. Fig. 2(b) illustrates only one of the 64 available styles for the 4/16-QAM Pe-Gray constellation.

For higher-order modulation, each layer-1 quadrant can be further divided into smaller sub-quadrants to accommodate more types of data streams. Each layer-1 quadrant consists of 4 subquadrants, known as layer-2 quadrants. From the layer-2 quadrant perspective, the 4/64-QAM Pe-Gray constellation's third group labeling bits constitutes 42 Gray mappings. These mappings share identical mapping orders for the 4^2 layer-2 quadrants. A layer-2 quadrant can be further equally divided into four subquadrants, called as layer-3 quarants. From the layer-3 quadrant perspective, the 4/256-QAM Pe-Gray constellation's fourth group labeling bits constitutes 4³ Gray mappings. These mappings share identical mapping orders for the 4^3 layer-3 quadrants, ..., from the perspective of the layer-(k-1) quadrant, the (k-1)-th group labeling bits of the $4/4^k$ -QAM Pe-Gray constellation, form 4^{k-1} Gray mappings with the same mapping orders for the 4^{k-1} layer-(k-1)quadrants. Thus V^k can be generated by relocating the center of the $Q^k(d_k)$ to each (k-1)-th layer constellation point. For $i, j = \{1, 2, \dots, 2^k\}$, the k-th group labeling bits, i.e., $v_{i,j}^k$, are then assigned based on the label of the constellation point of $Q^k(d_k)$ at its corresponding position. Additionally, $\{v^1_{i,j}, v^2_{i,j}, \cdots, v^{k-1}_{i,j}\}$ are determined based on the label of the (k-1)-th layer constellation point located at the shifted $Q^k(d_k)$. The labeling bits' difference between constellation points within each shifted $Q^k(d_k)$ is given by $v_{i,j}^k$. This approach can be used to construct structurally enhanced layers for the Pe-Gray constellation, which facilitates the creation of a 4/M-QAM Pe-Gray constellation for practical transmission.

The structured design process for the 4/M-QAM Pe-Gray constellation is denoted by the function $f(\cdot)$.

$$V^{1} = Q^{1}(d_{1}),$$

$$V^{2} = f(V^{1}, Q^{2}(d_{2})),$$

$$V^{3} = f(V^{2}, Q^{3}(d_{3})),$$

$$\vdots$$

$$V^{K} = f(V^{K-1}, Q^{K}(d_{K})).$$
(3)

Suppose that we have generated V^{k-1} and a layer-k 4-QAM Gray basic constellation matrix, i.e., $Q^k(d_k)$. Then, we can use this design rule to create V^k . Note that V^{k-1} consists of $2^{k-1} \times 2^{k-1}$ constellation points arranged in 2^{k-1} rows

and 2^{k-1} columns, as expressed as (4). The points in the same row share the same vertical coordinate, and points in the same column share the same horizontal coordinate. We can derive V^k using V^{k-1} and $Q^k(d_k)$ via the function $f(\cdot)$, i.e., $V^k = f(V^{k-1},Q^k(d_k))$, as shown in (5). The term $\mathbf{v}_{i,j}^{k-1}(x_{i,j},y_{i,j})\bar{\otimes}Q^k(d_k)$ means that the center of $Q^k(d_k)$ relocates to $\mathbf{v}_{i,j}^{k-1}(x_{i,j},y_{i,j})$, $i,j=\{1,2,\ldots,2^{k-1}\}$, resulting in the creation of new constellation points, while $\bar{\otimes}$ means shift and perform constellation point superimposed operation. The constellation point located at the i-th row and j-th column in V^{k-1} is labeled as $\mathbf{v}_{i,j}^{k-1}$ and has the coordinate pair $(x_{i,j},y_{i,j})$. The implementation details are provided in (6), where $[\cdot,\cdot]$ indicates bits splicing operation, e.g., [0010,01]=001001.

B. Properties of Superimposed Constellation

Theorem 1. The 4/M-QAM Pe-Gray constellation is utilized at the users, resulting in a Gray-mapped and unambiguous superimposed constellation at the relay.

Proof. First, consider the case that the users are modulated with the basic constellation. Assuming that the basic constellation used at the users is $Q^k(d_k)$, we can define $S^k(d_{s_k})$ as the layer-k basic superimposed constellation matrix with adjacent constellation points separated by d_{s_k} . To generate the basic superimposed constellation at the relay, we introduce the $g(\cdot)$ function in (7) for the generation process.

In this paper, $q_{i,j}^k(x_{i,j},y_{i,j}) \bar{\oplus} Q^k(d_k)$ is used to indicate that $Q^k(d_k)$ is moved to the position of $q_{i,j}^k(x_{i,j},y_{i,j})$ to generate superimposed constellation points, where $i,j=\{1,2\}$. The specific operation is given in (8), where \oplus represents bit-wise

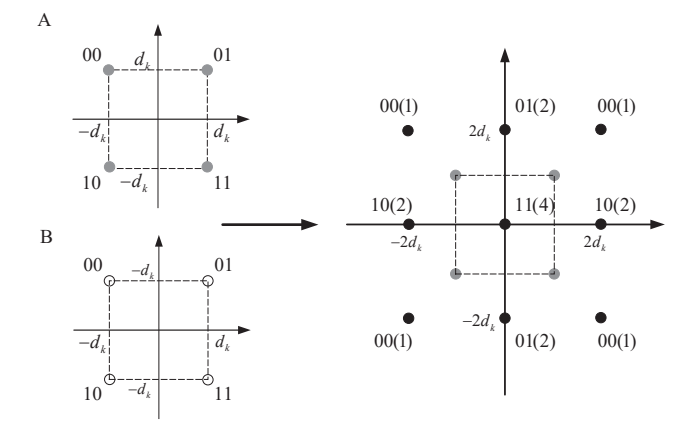


Fig. 6. Generation of the layer-k basic superimposed constellation at the relay.

XOR operation. Recall that the constellation matrix $Q^k(d_k)$ is also a 4-QAM Gray constellation, where adjacent constellation points differ by one bit and diagonal constellation points differ by two bits. Therefore, with (8), we can obtain the corresponding relationships as given in Table I. When 01/10 and 10/01 are used together, it indicates that if one is 01, the other is 10, and vice versa. In other words, they are mutually exclusive.

After applying the necessary labels and coordinates operations, we can derive $S^k(d_{s_k})$ and subsequently determine the corresponding basic superimposed constellation. A specific example of the generation of the layer-k basic superimposed constellation is depicted in Fig. 6. It is noteworthy that the figures in parentheses indicate the number of points in the

$$V^{k-1} = \begin{bmatrix} \mathbf{v}_{1,1}^{k-1}(x_{1,1}, y_{1,1}) & \mathbf{v}_{1,2}^{k-1}(x_{1,2}, y_{1,2}) & \cdots & \mathbf{v}_{1,2^{k-1}}^{k-1}(x_{1,2^{k-1}}, y_{1,2^{k-1}}) \\ \mathbf{v}_{2,1}^{k-1}(x_{2,1}, y_{2,1}) & \mathbf{v}_{2,2}^{k-1}(x_{2,2}, y_{2,2}) & \cdots & \mathbf{v}_{2,2^{k-1}}^{k-1}(x_{2,2^{k-1}}, y_{2,2^{k-1}}) \\ \vdots & \vdots & \ddots & \vdots \\ \mathbf{v}_{2^{k-1},1}^{k-1}(x_{2^{k-1},1}, y_{2^{k-1},1}) & \mathbf{v}_{2^{k-1},2}^{k-1}(x_{2^{k-1},2}, y_{2^{k-1},2}) & \cdots & \mathbf{v}_{2^{k-1},2^{k-1}}^{k-1}(x_{2^{k-1},2^{k-1}}, y_{2^{k-1},2^{k-1}}) \end{bmatrix}, \tag{4}$$

$$V^{k} = f(V^{k-1}, Q^{k}(d_{k}))$$

$$= \begin{bmatrix} \mathbf{v}_{1,1}^{k-1}(x_{1,1}, y_{1,1}) \bar{\otimes} Q^{k}(d_{k}) & \mathbf{v}_{1,2}^{k-1}(x_{1,2}, y_{1,2}) \bar{\otimes} Q^{k}(d_{k}) & \cdots & \mathbf{v}_{1,2^{k-1}}^{k-1}(x_{1,2^{k-1}}, y_{1,2^{k-1}}) \bar{\otimes} Q^{k}(d_{k}) \\ \mathbf{v}_{2,1}^{k-1}(x_{2,1}, y_{2,1}) \bar{\otimes} Q^{k}(d_{k}) & \mathbf{v}_{2,2}^{k-1}(x_{2,2}, y_{2,2}) \bar{\otimes} Q^{k}(d_{k}) & \cdots & \mathbf{v}_{2,2^{k-1}}^{k-1}(x_{2,2^{k-1}}, y_{2,2^{k-1}}) \bar{\otimes} Q^{k}(d_{k}) \\ \vdots & \vdots & \ddots & \vdots \\ \mathbf{v}_{2^{k-1},1}^{k-1}(x_{2^{k-1},1}, y_{2^{k-1},1}) \bar{\otimes} Q^{k}(d_{k}) & \mathbf{v}_{2^{k-1},2}^{k-1}(x_{2^{k-1},2}, y_{2^{k-1},2}) \bar{\otimes} Q^{k}(d_{k}) & \cdots & \mathbf{v}_{2^{k-1},2^{k-1}}^{k-1}(x_{2^{k-1},2^{k-1}}, y_{2^{k-1},2^{k-1}}) \bar{\otimes} Q^{k}(d_{k}) \end{bmatrix},$$

$$(5)$$

$$\mathbf{v}_{i,j}^{k-1}(x_{i,j}, y_{i,j}) \bar{\otimes} Q^k(d_k) = \begin{bmatrix} [\mathbf{v}_{i,j}^{k-1}, q_{1,1}^k](x_{i,j} - d_k, y_{i,j} + d_k) & [\mathbf{v}_{i,j}^{k-1}, q_{1,2}^k](x_{i,j} + d_k, y_{i,j} + d_k) \\ [\mathbf{v}_{i,j}^{k-1}, q_{2,1}^k](x_{i,j} - d_k, y_{i,j} - d_k) & [\mathbf{v}_{i,j}^{k-1}, q_{2,2}^k](x_{i,j} + d_k, y_{i,j} - d_k) \end{bmatrix},$$
(6)

$$S^{k}(d_{s_{k}}) = g(Q^{k}(d_{k}), Q^{k}(d_{k})) = \begin{bmatrix} q_{1,1}^{k}(-d_{k}, d_{k}) \bar{\oplus} Q^{k}(d_{k}) & q_{1,2}^{k}(d_{k}, d_{k}) \bar{\oplus} Q^{k}(d_{k}) \\ q_{2,1}^{k}(-d_{k}, -d_{k}) \bar{\oplus} Q^{k}(d_{k}) & q_{2,2}^{k}(d_{k}, -d_{k}) \bar{\oplus} Q^{k}(d_{k}) \end{bmatrix},$$
(7)

$$q_{i,j}^k(x_{i,j},y_{i,j})\bar{\oplus}Q^k(d_k) = \begin{bmatrix} (q_{i,j}^k \oplus q_{1,1}^k)(x_{i,j} - d_k, y_{i,j} + d_k) & (q_{i,j}^k \oplus q_{1,2}^k)(x_{i,j} + d_k, y_{i,j} + d_k) \\ (q_{i,j}^k \oplus q_{2,1}^k)(x_{i,j} - d_k, y_{i,j} - d_k) & (q_{i,j}^k \oplus q_{2,2}^k)(x_{i,j} + d_k, y_{i,j} - d_k) \end{bmatrix}.$$
(8)

user A	user B	relay	user A	user B	relay
$q_{1,1}^k(-d_k,d_k)$	$q_{1,1}^k(-d_k,d_k)$	$00(-2d_k, 2d_k)$	$q_{1,2}^k(d_k,d_k)$	$q_{1,1}^k(-d_k,d_k)$	$01/10(0,2d_k)$
$q_{1,1}^k(-d_k,d_k)$	$q_{1,2}^k(d_k,d_k)$	$01/10(0, 2d_k)$	$q_{1,2}^k(d_k,d_k)$	$q_{1,2}^k(d_k,d_k)$	$00(2d_k, 2d_k)$
$q_{1,1}^k(-d_k,d_k)$	$q_{2,1}^k(-d_k, -d_k)$	$10/01(-2d_k,0)$	$q_{1,2}^k(d_k,d_k)$	$q_{2,1}^k(-d_k,-d_k)$	11(0,0)
$q_{1,1}^k(-d_k,d_k)$	$q_{2,2}^k(d_k,-d_k)$	11(0,0)	$q_{1,2}^k(d_k,d_k)$	$q_{2,2}^k(d_k,-d_k)$	$10/01(2d_k,0)$
$q_{2,1}^k(-d_k,-d_k)$	$q_{1,1}^k(-d_k,d_k)$	$10/01(-2d_k,0)$	$q_{2,2}^k(d_k, -d_k)$	$q_{1,1}^k(-d_k,d_k)$	11(0,0)
$q_{2,1}^k(-d_k, -d_k)$	$q_{1,2}^k(d_k,d_k)$	11(0,0)	$q_{2,2}^k(d_k, -d_k)$	$q_{1,2}^k(d_k,d_k)$	$10/01(2d_k,0)$
$q_{2,1}^{k}(-d_k,-d_k)$	$q_{2,1}^k(-d_k, -d_k)$	$00(-2d_k, -2d_k)$	$q_{2,2}^k(d_k, -d_k)$	$q_{2,1}^k(-d_k, -d_k)$	$01/10(0, -2d_k)$
$q_{2,1}^k(-d_k,-d_k)$	$q_{2,2}^k(d_k,-d_k)$	$01/10(0, -2d_k)$	$q_{2,2}^k(d_k, -d_k)$	$q_{2,2}^k(d_k,-d_k)$	$00(2d_k, -2d_k)$

TABLE I
RELATIONSHIPS BETWEEN USER AND SUPERIMPOSED CONSTELLATIONS.

constellation where the coordinates overlap. By following this approach, we can identify the properties inherent to the basic superimposed constellation.

- 1) Distance: The separation distance between adjacent constellation points $d_{sk} = 2d_k$.
- 2) Symmetrical and unambiguous labels: The superimposed constellation has a symmetrical distribution of labels around both the real and imaginary axes, resulting in symmetrical labels. The labels of the constellation points with overlapping coordinates are identical, which can generate the unambiguous superimposed constellation.
- 3) Gray-mapped distribution: The basic superimposed constellation is Gray-mapped, where neighboring constellation points differ by only one bit.

Consequently, the 4-QAM Gray basic constellation is utilized at the users, resulting in a Gray-mapped basic superimposed constellation at the relay with symmetrical and unambiguous labels.

Then, we delve deeper into the case where the users utilize a 4/M-QAM Pe-Gray constellation. The 4/M-QAM Pe-Gray constellation design rule can be used to sequentially construct V^K by $Q^k(d_k)$, where $k=1,2,\ldots,K$ and $K=(\log_2 M)/2$. The Pe-Gray constellation has a layered structure and mapping properties that enable the creation of a superimposed constellation with its own layered structure and the same mapping order properties. From the superimposed constellation and the 4/M-QAM Pe-Gray constellation generations, it can deduce that the $C_R(\text{Pe-Gray})$ can be constructed recursively by $S^k(d_{s_k})$ via $f(\cdot), \ k=1,2,\ldots,K$. Let R^k denote the superimposed constellation matrix obtained by the constellation matrices of the previous k layers of the basic superimposed constellations. Therefore, the R^k can be recursively generated as

$$R^{1} = S^{1}(d_{s_{1}}),$$

$$R^{2} = f(R^{1}, S^{2}(d_{s_{2}})),$$

$$R^{3} = f(R^{2}, S^{3}(d_{s_{3}})),$$

$$\vdots$$

$$R^{K} = f(R^{K-1}, S^{K}(d_{s_{K}})).$$
(9)

Assume that the label of a constellation point in R^k is $\mathbf{r}^k = \{r^1, r^2, \cdots, r^k\}$, and $r^i \in \{00, 01, 10, 11\}$ denotes the XOR value of the *i*-th group of labeling bits of two constellation points from user A and B, $i = 1, 2, \ldots, k$. We refer to a group of 16 constellation points that form a

basic superimposed constellation as a cluster. The 16 new constellation points in \mathbb{R}^k generated by every shifted \mathbb{S}^k are called a layer-k cluster.

 $R^1 = S^1(d_{s_1})$ corresponds to the layer-1 basic superimposed constellation with the center located at (0,0) and contains a layer-1 cluster. By the properties of the basic superimposed constellation, R^1 is Gray-mapped and $d_{s_1} = 2d_1$.

 $R^2 = f(R^1, S^2(d_{s_2}))$ means that R^2 is created by shifting the center of $S^2(d_{s_2})$ to the location of each constellation point in R^1 . R^2 contains 4^2 layer-2 clusters, some of which overlap and share the same labels, thereby eliminating any confusion or ambiguity in the constellation. Applying the $f(\cdot)$ operation ensures that r^1 in each layer-2 cluster is identical, and r^2 is determined by the location of the point in $S^2(d_{s_2})$. Since $S^2(d_{s_2})$ is Gray-mapped, each layer-2 cluster in R^2 is internally Gray-mapped. Within each layer-2 cluster, r^2 has the same mapping order and symmetric labels, so the only difference between neighboring constellation points in adjacent layer-2 clusters is r^1 . The value of r^1 for each layer-2 cluster is determined by R^1 , which is also Graymapped. Consequently, the neighboring constellation points of adjacent layer-2 clusters differ in only one bit. In this case, the distance between constellation points in each layer-2 cluster is $d_{s_2}=2d_2$, and the distance between adjacent layer-2 clusters is $d_{out}^2 = d_{s_1} - 2d_{s_2}$. If $d_{out}^2 > 0$ (i.e., $\lambda_1 = d_2/d_1 < 1/2$), then the constellation is unambiguous. The layer-2 clusters follow the Gray mapping distribution both within and between them, which means that R^2 is also Gray-mapped.

 $R^3=f(R^2,S^3(d_{s_3}))$ is generated by moving the center of $S^3(d_{s_3})$ to each constellation point of R^2 , resulting in 4^4 layer-3 clusters within R^3 . Within each layer-3 cluster, r^3 is determined by $S^3(d_{s_3})$, while $\{r^1,r^2\}$ is determined by the R^2 constellation point located at the cluster's position. The distance between neighboring constellation points in every layer-3 cluster is $d_{s_3}=2d_3$, and the distance between adjacent clusters is $d_{out}^3=\min(d_{out}^2,2d_{s_2})-2d_{s_3}$. When $d_{out}^3>0$, there is no overlap between adjacent layer-3 clusters, avoiding ambiguity. Since both $S^3(d_{s_3})$ and R^2 have a Gray mapping distribution, R^3 is also Gray-mapped overall.

Based on the above analysis, (9) can be rewritten as

$$R^{K} = S^{1}(d_{s_{1}}) \bar{\otimes} S^{2}(d_{s_{2}}) \bar{\otimes} \cdots \bar{\otimes} S^{K}(d_{s_{K}}).$$
 (10)

Due to the condition that $d_{out}^i>0, i=2,3,\ldots,K$, the desired R^K is Gray-mapped. Thus, both $S^K(d_{s_K})$ and R^{K-1} can also be Gray-mapped. To ensure that R^{K-1} follows

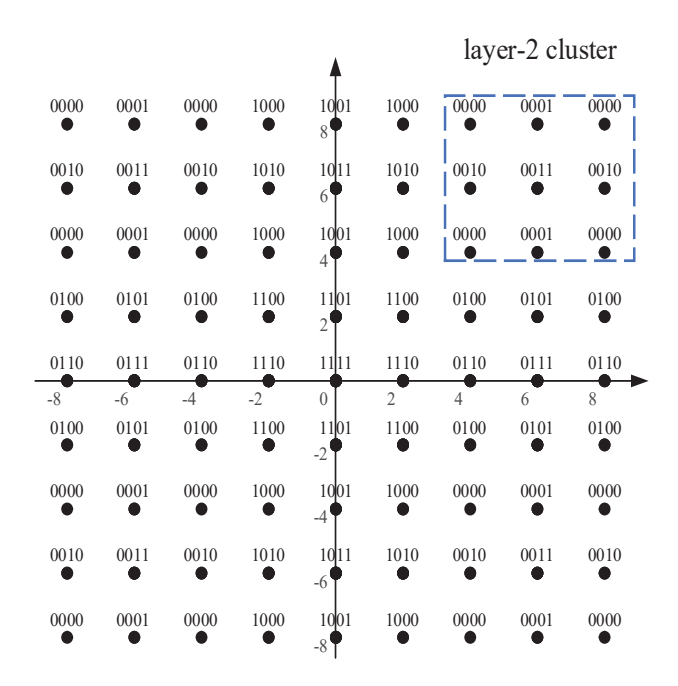


Fig. 7. Constellation diagram of C_R (Pe-Gray).

a Gray-mapping distribution, both $S^{K-1}(d_{s_{K-1}})$ and R^{K-2} are Gray-mapped. Similarly, both $S^2(d_{s_2})$ and R^1 are Gray-mapped, which can ensure the R^2 to be Gray-mapped.

From the design principle of the Pe-Gray constellation, it is essential to ensure that the basic constellations of all the layers are Gray-mapped. In addition, the enhanced layers can have the same mapping orders for each previous layer quadrant, while the constellation priority parameters meet the condition of $\lambda_i = d_{i+1}/d_i < 1/2, \ i = 1,2,\ldots,K-1$. Then, the condition that $d^i_{out} > 0$ guarantees non-overlapping adjacent layer-i clusters, $i = 2,3,\ldots,K$. By satisfying these criteria, the resulting superimposed constellation can be unambiguous and Gray-mapped. This property holds recursively. Fig. 7 shows the superimposed constellation at the relay obtained by using the 4/16-QAM Pe-Gray constellation shown in Fig. 2(b).

Moreover, this design method can be generalized to more users and non-network coded cases to construct the user mappings.

C. Achievable Rate Analysis

The different symbol mappings at the users leads to the different achievable rates in the PNC system [4]. In the case of HM-BICM-PNC, where users are equipped with a 4/M-QAM constellation, the achievable rate for the layer-k stream at the relay can be calculated by

$$Rate_{k} = 2 - \sum_{i=2*k-1}^{2*k} E\left[\log_{2} \frac{\sum_{z \in C_{R}(C)} p(y|z) p(z)}{\sum_{z \in C_{R}^{i,b}(C)} p(y|z) p(z)}\right], (11)$$

where E denotes the mathematical expectation and k = 1, 2, ..., K. $C_R(C)$ refers to the superimposed constellation at the relay when two users adopt the mapping C, while y

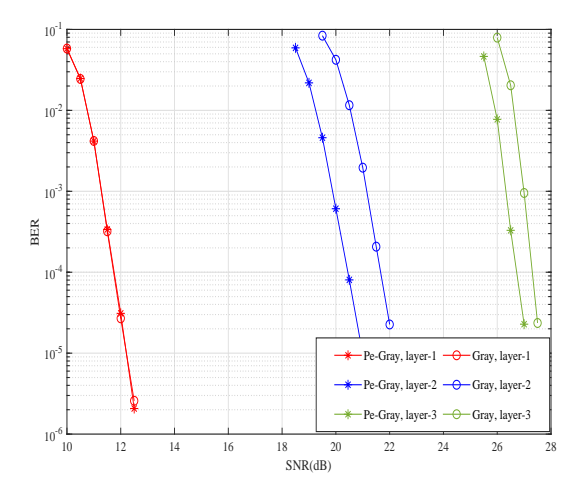


Fig. 10. BER curves of the layer-1, layer-2, and layer-3 data streams in the HM-BICM-PNC with the Gray and Pe-Gray constellations, $\lambda_1=\frac{1}{3}$ and $\lambda_2=\frac{1}{2}$. A 4/64-QAM modulation is considered.

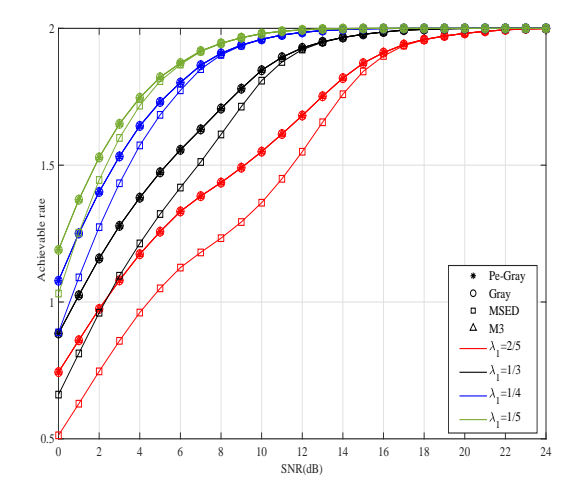


Fig. 11. Achievable rates of HP data streams with different λ_1 . A 4/16-QAM modulation is considered.

represents the received signal at the relay. Furthermore, z denotes a specific constellation point from $C_R(\mathbb{C})$. $b \in \{0,1\}$ represents the data bits transmitted by the users. The notation $C_R^{i,b}(\mathbb{C})$ corresponds to the set of constellation points in $C_R(\mathbb{C})$, where the i-th bit of the labeling bits is b.

IV. SIMULATION RESULTS

In this section, we show the simulated error performance and the achievable rate of HM-BICM-PNC systems with different constellations. Then, we examine the impact of constellation priority parameters on system performance. In the simulations, we consider regular (3,6) LDPC code with a code rate of 1/2 and a code length of 512 bits. We set the number of decoding iterations to 50.

A. Performance of Uncoded HM-PNC

Fig. 8 illustrates the BER curves for both HP and LP data streams in the un-coded HM-PNC systems with different constellations, i.e., MSED, M3, Gray, and the proposed Pe-Gray constellation. As shown in Fig. 8(a), the Pe-Gray

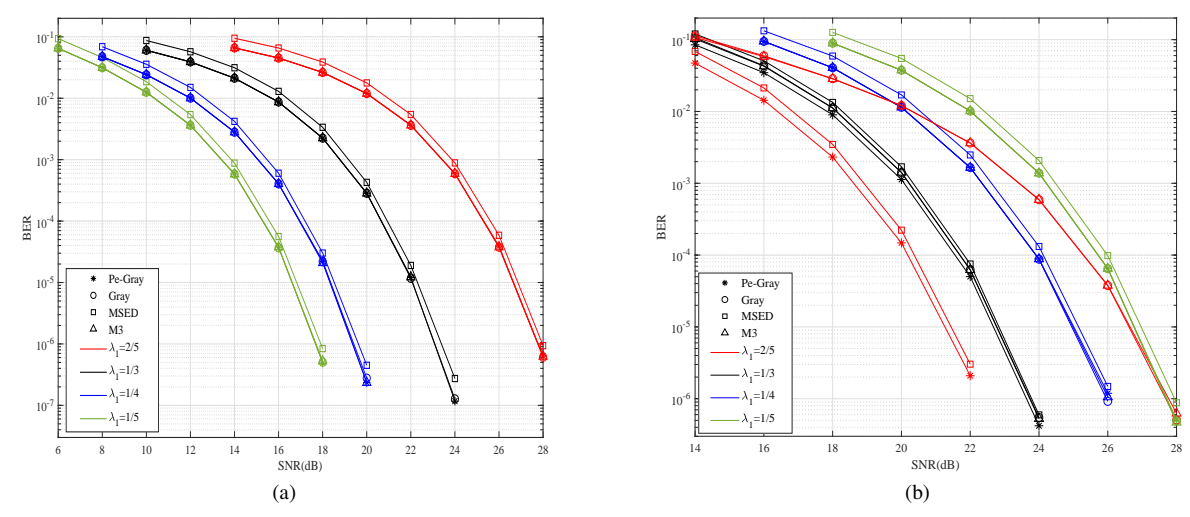


Fig. 8. Performance of un-coded PNC systems with different constellations. (a) HP data streams. (b) LP data streams. A 4/16-QAM modulation is considered.

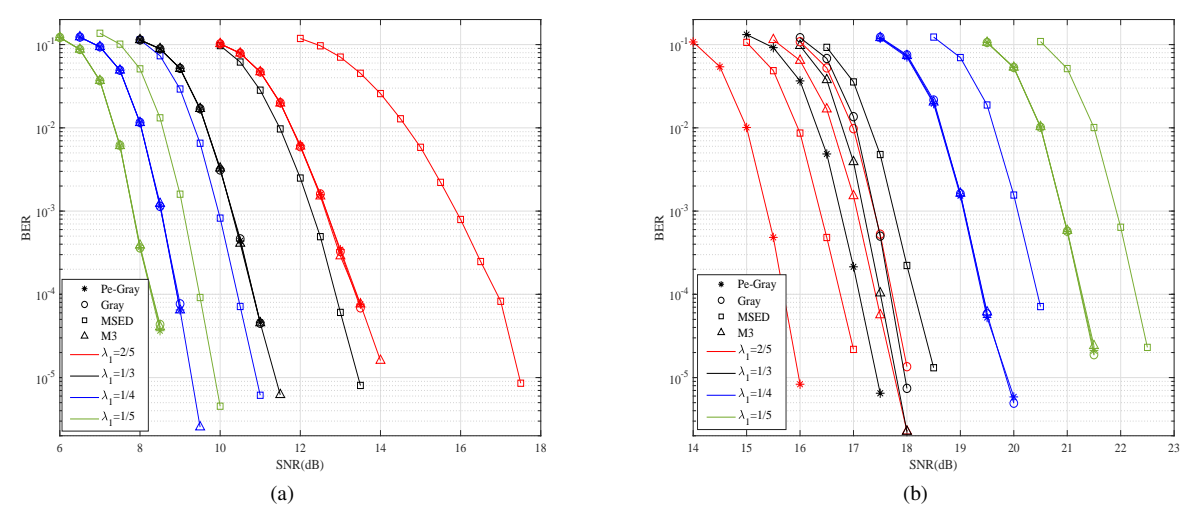


Fig. 9. BER curves of the HP and LP data streams in the HM-BICM-PNC with the MSED, M3, Gray, and Pe-Gray constellations. (a) HP data streams. (b) LP data streams. A 4/16-QAM modulation is considered.

constellation exhibits similar performance to the Gray and M3 constellations at the HP hierarchy, while outperforming the MSED constellation. The reason for this is that the HP labeling bits of $C_R(\text{Pe-Gray})$, $C_R(\text{Gray})$ and $C_R(\text{M3})$ are Gray-mapped at adjacent layer-2 clusters, whereas this is not the case for $C_R(\text{MSED})$.

In addition, Fig. 8(b) shows the performance of LP streams for these four constellations. It can be observed that Pe-Gray constellation performs better than the other constellations. This can be attributed to two properties of the LP labeling bits of $C_R(\text{Pe-Gray})$. First, the LP labeling bits are Gray-mapped within each layer-2 cluster. Second, the LP labeling bits of adjacent constellation points between adjacent layer-2 clusters are identical, which avoids the demapping ambiguity. Therefore, the likelihood of accurately decoding the LP labeling bits within the received signal can be enhanced. In contrast, none of the other three constellations can satisfy both the conditions, and then suffer from worse performance.

B. Performance of LDPC-coded HM-BICM-PNC

Fig. 9 illustrates the error performance of the HP and LP data streams in LDPC-coded HM-BICM-PNC with different 4/16-QAM constellations. In particular, we examine the impact of constellation priority parameter λ_1 on system performance. In Fig. 9(a), it is seen that for $\lambda_1 = 1/5, 1/4, 1/3, 2/5$, the Pe-Gray constellation can achieve excellent HP performance, similar to the Gray and M3 constellations, with remarkable gains of 1.2, 1.6, 2, and 3.4 dB over MSED at a BER of 1×10^{-4} , respectively. Fig. 9(b) further presents the BER performance of LP data streams. It shows that for $\lambda_1 = 1/5, 1/4$, the Pe-Gray, Gray, and M3 exhibit comparable LP performance and achieve a performance gain of 1.1 dB over MSED at a BER of 1×10^{-4} . In particular, for $\lambda_1 = 1/3$, the Pe-Gray constellation can achieve a gain of more than 0.5 dB over the M3, Gray, and MSED. Moreover, as λ_1 increases, i.e., $\lambda_1 = 2/5$, the proposed Pe-Gray exhibits superior LP performance, outperforming the other three constellations by up to 1.1, 1.7, and 2 dB, respectively, at a BER of 1×10^{-4} . These results demonstrate the effectiveness of our proposed

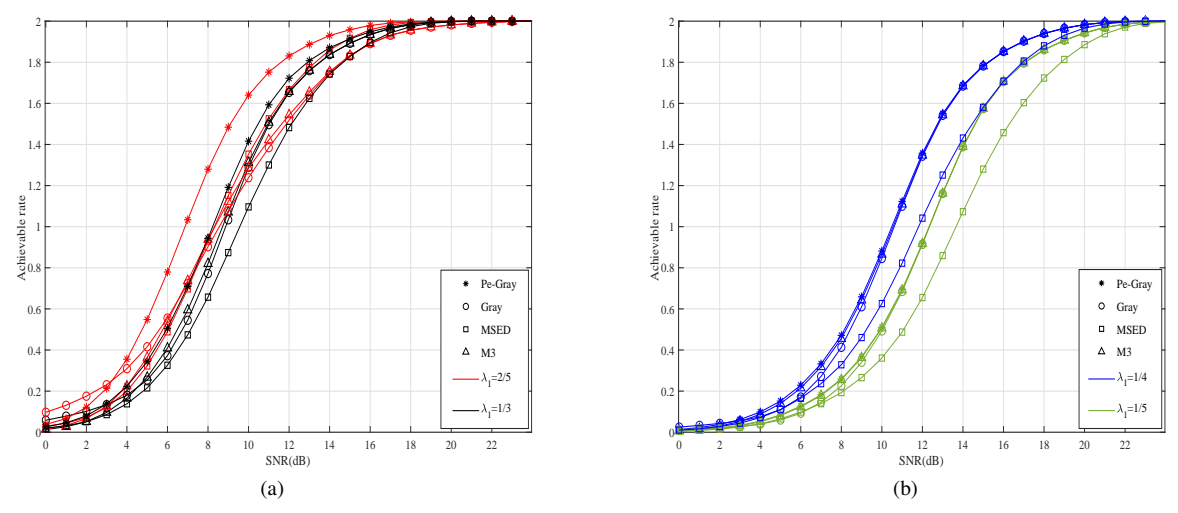


Fig. 12. Achievable rates of LP data streams with different λ_1 . (a) $\lambda_1=2/5,1/3$ (b) $\lambda_1=1/4,1/5$. A 4/16-QAM modulation is considered.

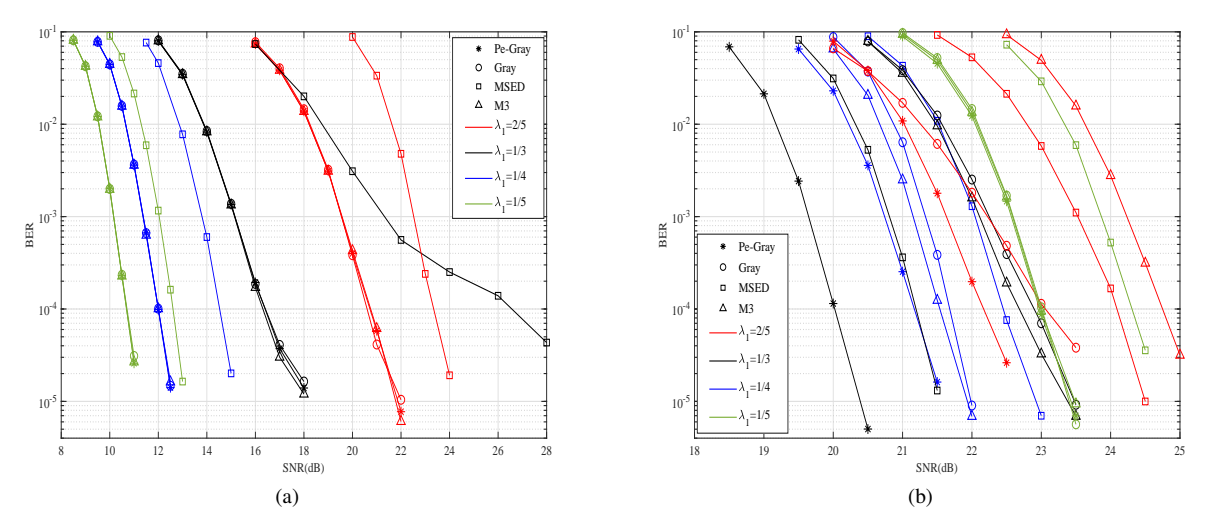


Fig. 13. BER curves of the HP and LP data streams in the HM-BICM-PNC with the MSED, M3, Gray, and Pe-Gray constellations in power-imbalanced channels. (a) HP data streams. (b) LP data streams. A 4/16-QAM modulation is considered.

approach.

The differences in LP performance can be attributed to variations in the distribution of LP labeling bits across the superimposed constellation, as well as fluctuations in the value of λ_1 . Unlike the other three constellations, $C_R(\text{Pe-Gray})$ exhibits Gray-mapped LP labeling bits within each layer-2 cluster, which share the same values for neighboring constellation points in adjacent layer-2 clusters. The LP performance is also affected by λ_1 . The value of λ_1 determines the numerical relationship between d_{out}^2 and d_{s_2} . Recall that the parameter d_{out}^2 represents the distance between adjacent layer-2 clusters, and d_{s_2} denotes the distance between neighboring constellation points within the layer-2 clusters. According to Theorem 1's proof, $d_{out}^2=2d_1-4d_2,\ d_{s_2}=2d_2.$ Thus, the following relationship can be established: $0\leq \lambda_1<1/3,\ d_{out}^2>d_{s_2};$ $\lambda_1=\frac{1}{3},\,d_{out}^2=d_{s_2};\,1/3<\lambda_1<1/2,\,d_{out}^2< d_{s_2}.$ Increasing λ_1 leads to a decrease in the value of d_{out}^2 , resulting in closely positioned layer-2 clusters. In this scenario, the distribution of LP labeling bits between adjacent layer-2 clusters determines the disparity in LP performance. Specifically, the LP labeling

bits of $C_R(\text{Pe-Gray})$ remain consistent between adjacent layer-2 clusters, enhancing the resistance of received signals to noise interference. Consequently, the LP labeling bits of the other three constellations are more susceptible to errors compared to the Pe-Gray constellation. Conversely, when λ_1 decreases and d_{out}^2 increases, the received signals between layer-2 clusters become less susceptible to noise interference. In this case, the distribution of LP labeling bits within the layer-2 cluster is the primary factor influencing LP performance. The Pe-Gray constellation demonstrates superior LP performance due to the distinctive characteristics of its LP labeling bits of $C_R(\text{Pe-Gray})$. These bits are identical between adjacent layer-2 clusters and follow a Gray-mapped distribution within each layer-2 cluster.

As shown in Figs. 8 and 9, the performance gain of the Pe-Gray over the traditional mappings in the coded system is larger than that in the uncoded system. It is due to that the Pe-Gray has fewer demodulation errors, which can be more easily corrected by the subsequent channel decoding.

To show the generality of the proposed design, we construct

a 4/64-QAM Pe-Gray constellation, which is capable of processing three data streams with $\lambda_1=1/3$ and $\lambda_2=1/3$. As depicted in Fig. 10, the proposed Pe-Gray exhibits superior performance in both layer-2 and layer-3 data streams as compared to the conventional Gray constellation, while retaining excellent layer-1 performance. Also note that the Pe-Gray achieves gains of 1.3 and 0.6 dB for the layer-2 and layer-3 streams, respectively, over the Gray constellation. Thus, the proposed Pe-Gray can maintain its advantage in HM-BICM-PNC with high-order modulations.

C. Comparison of Achievable HM-PNC Rates

Fig. 11 and Fig. 12 show the achievable rates of HP and LP data streams of Pe-Gray, Gray, M3 and MSED constellations with different λ_1 in 4/16-QAM HM-BICM-PNC, respectively. As we can see, the proposed Pe-Gray constellation shows excellent achievable rate in the HP hierarchy and outperforms other three constellations in the LP hierarchy. Notably, the BER performance and achievable rate exhibit a consistent pattern, providing confidence in the accuracy of the BER simulation results.

D. Performance of HM-BICM-PNC over Power-imbalanced Channels

To evaluate the proposed method in more generalized cases, Fig. 13 shows the error performance of the HP and LP data streams in HM-BICM-PNC with different constellations over a power-imbalanced channel of $(h_A, h_B) = (1.3, 0.7)$. From Fig. 13(a), we can see that the Pe-Gray constellation performs almost the same as that of the Gray and M3 constellations for $\lambda_1 = 1/5, 1/4, 1/3, 2/5$. It is similar to the comparison over the power-balanced channel in Fig. 9. Moreover, the Pe-Gray outperforms the MSED for all values of λ_1 , achieving significant gains of more than 2 dB, at a BER of 1×10^{-4} . On the other hand, Fig. 13(b) shows the superior performance of the Pe-Gray constellation in the LP stream. For $\lambda_1 = 1/3$, the Pe-Gray can obtain performance gains of 1.2, 2.6 and 2.8 dB over the MSED, M3, and Gray, respectively. Similarly, for $\lambda_1 = 1/4$, the Pe-Gray outperforms the other three constellations by 0.4 dB. As $\lambda_1 = 2/5$, the Pe-Gray also surpasses the Gray, MSED, and M3 constellations by 0.8, 1.9, and 2.5 dB, respectively. When $\lambda_1 = 1/5$, the Pe-Gray, Gray, and M3 has comparable LP performance, which achieve a gain of 1.3 dB over the MSED. Hence, in the case of unequal-power channels, the proposed constellation still maintains the performance superiority. It also suggests that the proposed scheme obtains the enhanced robustness against power imbalances and can perform efficiently in practical fading scenarios.

E. Performance of HM-BICM-PNC over Fading Channels

To assess the proposed mapping over more generalized scenarios, Fig. 14 illustrates the BER performance of both HP and LP data streams in HM-BICM-PNC systems over Rayleigh fading channels, where h_A and h_B are random complex numbers. As shown in Fig. 14(a), the Pe-Gray exhibits

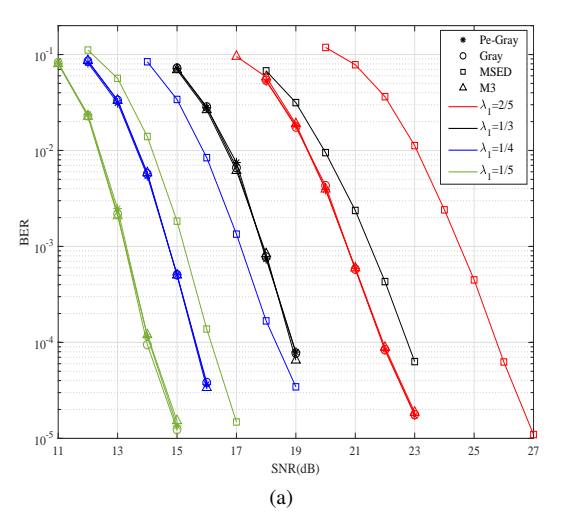
comparable performance to the other constellations. It achieves notable performance gains of more than 2 dB over the MSED at a BER of 1×10^{-4} . Fig. 14(b) shows the BER performance of LP data streams. It shows that for $\lambda_1=2/5,1/3$, the PeGray can achieve gains of 0.3 dB over the other constellations. For $\lambda_1=1/4$, this gain is increased to more than 1 dB. For $\lambda_1=1/5$, Pe-Gray and Gray constellations perform similarly, which outperform M3 and MSED by 0.4 dB. Therefore, the Pe-Gray constellation remains a performance advantage in the fading channels.

V. CONCLUSIONS

In this paper, we propose a novel 4/M-QAM constellation design, i.e., Pe-Gray constellation, for the HM-BICM-PNC. In this way, we can have the superimposed constellations that are Gray-mapped, which differ by only one bit at neighboring points. In particular, we derive the design criterion for Pe-Gray constellation to ensure the Gray-mapped constellations superimposed at the relay. Furthermore, the achievable rate analysis and simulation results show that for both 4/16-QAM and 4/64-QAM, the proposed Pe-Gray constellation can obtain significant performance gains over the conventional M3, Gray, and MSED constellations in the LP layers, while achieving an excellent layer-1 HP performance in AWGN channels. Also, as constellation priority parameter increases, the performance gain can be up to 2 dB at high SNR region. In addition, we conduct extensive simulations to evaluate the error performance over the power-imbalanced channels. The proposed Pe-Gray still outperforms the conventional ones by more than 1.5 dB. It suggests that the proposed constellation has enhanced robustness against the power-unequal effect, i.e., performs much better over generalized fading channels. Moreover, the performance-bound derivation for HM-PNC can help to assess the performance of the proposed mapping. We believe that this topic is interesting and deserves further exploration.

REFERENCES

- [1] S. Zhang, S. C. Liew, and P. P. Lam, "Hot topic: Physical-layer network coding," in *Proc. MobiCom, Los Angeles, USA*, 2006, pp. 23–29.
- [2] P. Popovski and H. Yomo, "The anti-packets can increase the achievable throughput of a wireless multi-hop network," in *Proc. IEEE Int. Conf. Commun.*, vol. 9, 2006, pp. 3885–3890.
- [3] L. You, S. C. Liew, and L. Lu, "Reliable physical-layer network coding supporting real applications," *IEEE Trans. Mob. Comput.*, vol. 16, no. 8, pp. 2334–2350, 2017.
- [4] P. Chen, S. C. Liew, and L. Shi, "Bandwidth-efficient coded modulation schemes for physical-layer network coding with high-order modulations," *IEEE Trans. Commun.*, vol. 65, no. 1, pp. 147–160, 2016.
- [5] H. Lei, X. She, K.-H. Park, I. S. Ansari, Z. Shi, J. Jiang, and M.-S. Alouini, "On Secure CDRT with NOMA and Physical-Layer Network Coding," *IEEE Trans. Commun.*, vol. 71, no. 1, pp. 381–396, 2023.
- [6] Q. T. Sun, J. Yuan, T. Huang, and K. W. Shum, "Lattice network codes based on Eisenstein integers," *IEEE Trans. Commun.*, vol. 61, no. 7, pp. 2713–2725, 2013.
- [7] Z. Wang, L. Liu, S. Zhang, P. Dong, Q. Yang, and T. Wang, "PNC Enabled IIoT: A General Framework for Channel-Coded Asymmetric Physical-Layer Network Coding," *IEEE Trans. Wireless Commun.*, vol. 21, no. 12, pp. 10335–10350, 2022.
- [8] H. Sun, C. Dong, S. X. Ng, and L. Hanzo, "Five decades of hierarchical modulation and its benefits in relay-aided networking," *IEEE Access*, vol. 3, pp. 2891–2921, 2015.
- [9] P. K. Vitthaladevuni and M.-S. Alouini, "A recursive algorithm for the exact BER computation of generalized hierarchical QAM constellations," *IEEE Trans. Inf. Theory*, vol. 49, no. 1, pp. 297–307, 2003.



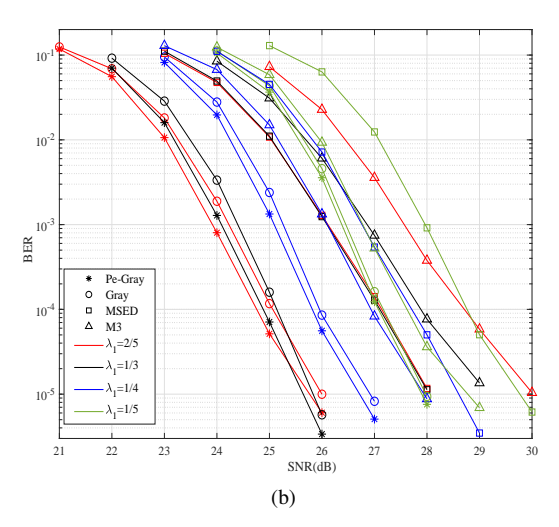


Fig. 14. BER curves of the HP and LP data streams in the HM-BICM-PNC with the MSED, M3, Gray, and Pe-Gray constellations in fading channels. (a) HP data streams. (b) LP data streams. A 4/16-QAM modulation is considered.

- [10] M. J. Hossain, P. K. Vitthaladevuni, M.-S. Alouini, V. K. Bhargava, and A. J. Goldsmith, "Adaptive hierarchical modulation for simultaneous voice and multiclass data transmission over fading channels," *IEEE Trans. Veh. Technol.*, vol. 55, no. 4, pp. 1181–1194, 2006.
- [11] C. Hausl and J. Hagenauer, "Relay communication with hierarchical modulation," *IEEE Commun. Lett.*, vol. 11, no. 1, pp. 64–66, 2007.
- [12] J. M. Park, S.-L. Kim, and J. Choi, "Hierarchically modulated network coding for asymmetric two-way relay systems," *IEEE Trans. Veh.r Technol.*, vol. 59, no. 5, pp. 2179–2184, 2010.
- [13] H. Jiang and P. A. Wilford, "A hierarchical modulation for upgrading digital broadcast systems," *IEEE Trans. Broadcast.*, vol. 51, no. 2, pp. 223–229, 2005.
- [14] M.-k. Chang and S.-y. Lee, "Performance analysis of cooperative communication system with hierarchical modulation over rayleigh fading channel," *IEEE Trans. Wireless Commun.*, vol. 8, no. 6, pp. 2848–2852, 2009.
- [15] G. Caire, G. Taricco, and E. Biglieri, "Bit-interleaved coded modulation," *IEEE Trans. Inf. Theory*, vol. 44, no. 3, pp. 927–946, 1998.
- [16] J. Wu, "Non-uniform and large distance constellation design for hierarchical modulation," in *Proc. IEEE Int. Conf. Commun. (ICC)*. IEEE, 2010, pp. 1–5.
- [17] Z. Yang, Y. Fang, G. Han, and K. M. S. Huq, "Spatially coupled protograph LDPC-coded hierarchical modulated BICM-ID systems: A promising transmission technique for 6G-enabled Internet of Things," *IEEE Internet Things J.*, vol. 8, no. 7, pp. 5149–5163, 2020.
- [18] S. N. Awny, C. C. Tsimenidis, J. Chambers, and S. Y. Le Goff, "Performance analysis of PLNC using hierarchical modulation," in 2017 25th EUSIPCO. IEEE, 2017, pp. 121–125.
- [19] M. Tang, J. Chen, Y. Zhang, and Y. Zhang, "Performance analysis for physical-layer network coding with hierarchical modulation," in 2016 8th IEEE ICCSN. IEEE, 2016, pp. 33–37.
- [20] H. J. Yang, Y. Choi, and J. Chun, "Modified high-order PAMs for binary coded physical-layer network coding," *IEEE Commun. Lett.*, vol. 14, no. 8, pp. 689–691, 2010.
- [21] M. Noori and M. Ardakani, "On symbol mapping for binary physicallayer network coding with PSK modulation," *IEEE Trans. Wireless Commun.*, vol. 11, no. 1, pp. 21–26, 2011.
- [22] R. Y. Chang, S.-J. Lin, and W.-H. Chung, "Symbol and bit mapping optimization for physical-layer network coding with pulse amplitude modulation," *IEEE Trans. Wireless Commun.*, vol. 12, no. 8, pp. 3956– 3967, 2013.
- [23] L. Shi, S. C. Liew, and L. Lu, "On the subtleties of q-pam linear physical-layer network coding," *IEEE Trans. Inf. Theory*, vol. 62, no. 5, pp. 2520–2544, 2016.
- [24] R. Gallager, "Low-density parity-check codes," IRE Trans. Inf. Theory, vol. 8, no. 1, pp. 21–28, Jan. 1962.
- [25] S. Zhang and S.-C. Liew, "Channel coding and decoding in a relay system operated with physical-layer network coding," *IEEE J.Sel. Areas Commun.*, vol. 27, no. 5, pp. 788–796, 2009.

- [26] T. Huang, T. Yang, J. Yuan, and I. Land, "Design of irregular repeataccumulate coded physical-layer network coding for gaussian two-way relay channels," *IEEE Trans. Commun.*, vol. 61, no. 3, pp. 897–909, 2013.
- [27] P. Chen, L. Shi, Y. Fang, F. C. M. Lau, and J. Cheng, "Rate-diverse multiple access over gaussian channels," *IEEE Trans. Wireless Commun.*, vol. 22, no. 8, pp. 5399–5413, 2023.
- [28] P. Chen, L. Shi, S. C. Liew, Y. Fang, and K. Cai, "Channel decoding for nonbinary physical-layer network coding in two-way relay systems," *IEEE Trans. Veh. Technol.*, vol. 68, no. 1, pp. 628–640, 2018.
- [29] E. Agrell, J. Lassing, E. G. Strom, and T. Ottosson, "On the optimality of the binary reflected gray code," *IEEE Trans. Inf. Theory*, vol. 50, no. 12, pp. 3170–3182, 2004.
- [30] Q. Li, J. Zhang, L. Bai, and J. Choi, "Performance analysis and system design for hierarchical modulated BICM-ID," *IEEE Trans. Wireless Commun.*, vol. 13, no. 6, pp. 3056–3069, 2014.
- [31] H. Huang and Y. Tsai, "Protection-level-exchanging hierarchical modulation for multiresolution services under decode-and-forward cooperative networks," *IEEE Trans. Veh. Technol.*, vol. 66, no. 8, pp. 6742–6753, 2017.
- [32] S. S. Ullah, S. C. Liew, G. Liva, and T. Wang, "Short-packet physical-layer network coding," *IEEE Trans. Commun.*, vol. 68, no. 2, pp. 737–751, 2019.
- [33] S. S. Ullah, S. C. Liew, G. Liva, and T. Wang, "Implementation of short-packet physical-layer network coding," *IEEE Trans. Mobile Comput.*, vol. 22, no. 1, pp. 284–298, 2021.
- [34] J. Tan, Q. Wang, C. Qian, Z. Wang, S. Chen, and L. Hanzo, "A reduced-complexity demapping algorithm for BICM-ID systems," *IEEE Trans. Veh. Technol.*, vol. 64, no. 9, pp. 4350–4356, 2014.
- [35] J. Chen, A. Dholakia, E. Eleftheriou, M. P. Fossorier, and X.-Y. Hu, "Reduced-complexity decoding of LDPC codes," *IEEE Trans. Commun.*, vol. 53, no. 8, pp. 1288–1299, 2005.
- [36] C. Stierstorfer and R. F. Fischer, "(Gray) mappings for bit-interleaved coded modulation," in *Proc. 2007 IEEE VTCSpring*. IEEE, 2007, pp. 1703–1707.
- [37] M. Vameghestahbanati, I. D. Marsland, R. H. Gohary, and H. Yanikomeroglu, "Multidimensional constellations for uplink SCMA systemsA comparative study," *IEEE Commun. Surveys Tuts.*, vol. 21, no. 3, pp. 2169–2194, 2019.
- [38] E. Agrell, J. Lassing, E. G. Strom, and T. Ottosson, "Gray coding for multilevel constellations in Gaussian noise," *IEEE Trans. Inf. Theory*, vol. 53, no. 1, pp. 224–235, 2006.



Pingping Chen (Senior Member, IEEE) is currently a Professor in Fuzhou University, China. He received the Ph.D. degree in electronic engineering, Xiamen University, China, in 2013. From May 2012 to September 2012, he was a Research Assistant in electronic and information engineering with The Hong Kong Polytechnic University, Hong Kong. From January 2013 to January 2015, he was a Postdoctoral Fellow at the Institute of Network Coding, Chinese University of Hong Kong, Hong Kong. From July 2016 to July 2017, he was a Postdoctoral

Fellow at Singapore University of Technology and Design. His primary research interests include channel coding, data storage, joint source and channel coding, and network coding.



Yuchen Lin received the B.Sc. degree in electronic information engineering from Fuzhou University, Fujian, China, in 2021, where he is currently pursuing the M.Sc. degree with the Department of Physics and Information Engineering. His research interests include hierarchical modulation, constellation design, and their applications to wireless communications.



Hanxin Zeng received the M.S. degree in communication and information system from Fuzhou University, Fujian, China in 2018, where he is currently pursuing the Ph.D degree with the Department of Physics and Information Engineering. His research interests include Massive MIMO detection, LDPC decoding, and their applications to wireless communications.



Yi Fang (Senior Member, IEEE) received the Ph.D. degree in communication engineering from Xiamen University, China, in 2013. From May 2012 to July 2012, he was a Research Assistant in electronic and information engineering with The Hong Kong Polytechnic University, Hong Kong. From September 2012 to September 2013, he was a Visiting Scholar in electronic and electrical engineering with University College London, U.K. From February 2014 to February 2015, he was a Research Fellow at the School of Electrical and Electronic Engineering,

Nanyang Technological University, Singapore. He is currently a Full Professor and the Vice Dean of the School of Information Engineering, Guangdong University of Technology, China. His current research interests include information and coding theory, spread-spectrum modulation, and cooperative communications. He served as the Publicity Co-Chair for the International Symposium on Turbo Codes and Iterative Information Processing 2018.



Zhaopeng Xie received the Ph.D. degree in communication and information system from Fuzhou University, Fujian, China, in 2023. He is currently an lecturer with the school of Advanced Manufacturing, Fuzhou University, China. His primary research in terests include joint source and channel coding, signal processing for wireless communication, channel coding, physical network coding.



Francis C. M. Lau (Fellow, IEEE) received the B.Eng. degree (Hons.) in electrical and electronic engineering and the Ph.D. degree from Kings College London, University of London, U.K.He is a Professor with the Department of Electronic and Information Engineering, The Hong Kong Polytechnic University, Hong Kong. He is a coauthor of two research monographs. He is also a co-holder of six U.S. patents. He has published more than330 papers. His main research interests include channel coding, cooperative networks, wireless sensor net-

works, chaos-based digital communications, applications of complex network theories, and wireless communications. Prof. Lau is a fellow of IET. He was a co-recipient of the one Natural Science Award from the Guangdong Provincial Government, China; eight Best/Outstanding Conference Paper Awards; one Technology Transfer Award; two Young Scientist Awards from International Union of Radio Science; and one FPGA Design Competition Award. He was the General Co-chair of International Symposium on Turbo Codes and Iterative Information Processing in 2018 and the Chair of Technical Committee on Nonlinear Circuits and Systems, IEEE Circuits and Systems Society, from 2012 to 2013. He served as an Associate Editor for IEEE TRANSACTIONS ON CIRCUITS AND SYSTEMS II: EXPRESS BRIEFS, from 2004 to 2005 and from 2015 to 2019, IEEE TRANSACTIONS ON CIRCUITS AND SYSTEMS I: REGULAR PAPERS, from 2006 to 2007, and IEEE Circuits and Systems Magazine, from 2012 to 2015. He has been a Guest Associate Editor of International Journal of Bifurcation and Chaos in Applied Sciences and Engineering, since 2010.